Mechanical properties and fractography of cement-based composites reinforced by natural piassava and jute fibers

F. P. Teixeira[1], V. N. Lima[2], D. J. C. Moutinho[3], R. T. Fujiyama[1]*

[1]*Universidade Federal do Pará, Faculty of Mechanical Engineering, 66075-110, Belém, PA, Brazil*

[2]*Pontifícia Universidade Católica do Rio de Janeiro, Department of Civil and Environmental Engineering, 22451-900, Rio de Janeiro, RJ, Brazil*

[3]*Instituto Federal de Educação, Ciência e Tecnologia do Pará, 68515-000, Parauapebas, PA, Brazil*

Abstract

Today's demand for environmentally friendly and energy-efficient solutions to the construction industry has driven researchers to match natural resources with traditional technics to develop new building technologies. However, there are literature limitations about the correlation of fiber-matrix interface with the failure of natural fibers in mortar plates, which hinders the advances in understanding the mechanical properties of these composites on a structural scale. The present work investigated the mechanical behavior and fractography of cement-based composites reinforced by natural piassava and jute fibers. The experimental program included flexural tests and scanning electron microscopy analyzes. The developed composite material under flexural tests demonstrated a flexural-softening behavior, reaching up to 5.7 MPa, with a considerable residual strength ruled by toughness. The fractography analyses presented the fibers' structure after mechanical tests and how effective its interaction with the matrix was. The piassava fibers demonstrated significant adherence when favorably oriented, while jute fibers (used as twisted yarn) provided voids in the composite by its partial matrix-covered filaments.

Keywords: cement-based composites, natural fibers, mechanical behavior, fractography.

INTRODUCTION

The cracking of cementitious materials usually occurs at very low tensile stresses because this frictional material has a remarkably low tensile strength (approximately 7-11% of its compressive strength) [1]. For this reason, cementitious materials are generally classified as 'fragile material'. The typical stress-strain relationship for a stressed fiber-reinforced cementitious (FRC) element demonstrates that it has two different behaviors before and after crack initiation. As shown in Fig. 1, the resistance to cracking and post-cracking of an FRC is characterized based on these behaviors. It is often thought that this unfavorable behavior of cementitious materials in the post-crack phase can be altered by the incorporation of discontinuous fibrous reinforcement. However, the benefits of fibers in the pre-crack stage are not well understood, and it is generally defined that fibers do not contribute to this stage [2-6]. According to Naaman [4], the strength of the matrix controls the crack strength, and the fiber-matrix interfacial bond dominates the post-crack strength. It is well accepted that the inclusion of fibers in a brittle matrix considerably improves its post-cracking performance; however, Gray and Johnson [7] reported that the modulus of rupture (tensile strength and first crack) and the associated absorbed energy of a fiber-reinforced concrete can be improved dramatically with the increase in the fiber-matrix bond strength. This fact can be visibly observed in graphs of toughness by crack mouth opening displacement or toughness by deflection. In addition, these researchers observed that the final tensile strength, the deformation capacity, and the absorbed energy of fiber-reinforced cementitious composites are improved by increasing the shear strength of the fiber-matrix interface.

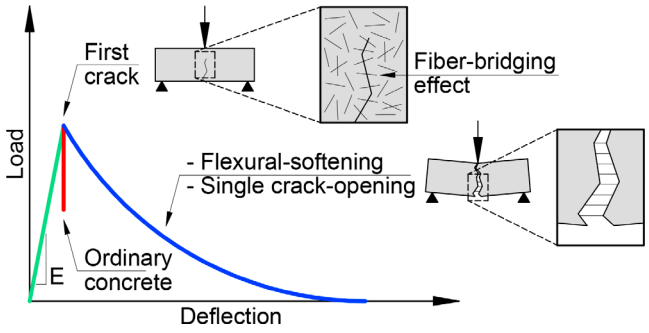

Figure 1: Mechanics and micromechanics of FRC beam.

Generally, fiber-matrix interactions govern the mechanical properties of the cementitious composite [7-11]. These properties include: 1) resistance to compressive, tensile, and bending strengths, 2) modulus of elasticity, 3) ultimate strain fracture toughness, 4) resistance to impact and seismic, 5) ductility, and 6) durability [7, 9, 11, 12]. It has been proven that the FRC with superior mechanical properties could not be developed unless the interfacial bond of the fiber-matrix was at least equal to the tensile strength of the matrix [4]. However, the remarkably strong fiber-matrix

**felipe.pinheiro.teixeira@gmail.com*
https://orcid.org/0000-0002-9108-7345

bond does not guarantee the production of ductile FRC, which indicates the importance of the matrix and fiber properties. The tensile strength of the fiber, the microstructure of the matrix, and the length/alignment in relation to the applied tension/fiber content are important for the fiber's ability to mitigate cracks [9]. For the mechanical characterization of fiber-reinforced composite, direct and indirect experimental methods were developed to quantify the fiber-matrix bond [13, 14]. In direct methods, the behavior of the fiber-matrix bond is evaluated by measuring the uniaxial tensile load and the corresponding slip during the pullout of the fiber from a cementitious matrix [7, 9, 14-17]. On the other hand, in indirect methods, the fiber-matrix bond strength is evaluated based on the mechanical property (mainly the flexural strength) of the cementitious composites [18-21].

In this field, natural fibers are a promising resource for the development of high-performance cementitious composites. This kind of fiber presents significant tensile strength and strain capacity [22-28], making it an economical and eco-friendly alternative to conventional reinforcement systems. In the last years, many authors [29-31] have mechanically evaluated the use of different natural fibers as reinforcement for cement-based composites and presented a positive perspective of its application. Soltan et al. [32] studied cementitious composites reinforced with curauá short fiber, with the average length varying between 10 and 20 mm. The tensile strain-softening behavior was observed for the composite reinforced with 2% of volume fraction of fibers. Fiber bridging capacity with 2% by volume was not sufficient to generate any multiple cracking behaviors. Instead, these specimens failed by the slow opening of the first crack formed in the matrix. However, the 4.4% of volume fraction reinforced composites presented the distributed micro-cracking and strain-hardening behavior, as previously mentioned by Fantilli et al. [33]. Hwang et al. [34] examined the effect of adding random, short coconut fibers to cementitious composites on the mechanical properties, using different volume fractions (0, 1%, 2.5%, and 4%). The increase in coconut fiber content from 0 to 4% increased the flexural strength of the cementitious sheet and the modulus of rupture from 5.2 to 7.4 MPa and from 6.8 to 8.8 MPa, respectively. The addition of coconut fiber to the composite samples enhanced the first-crack deflection and the toughness indices remarkably. The first-crack deflection increased from 0.23 to 0.55 mm when the coconut fiber volume fraction rose from 0 to 4%. In their work about cementitious composites reinforced with short curauá fibers (20 mm in length and 4% by volume), Zukowski et al. [35] observed that the composite presented a multiple-cracking pattern (from 2 to 4) and the increased strain capacity in a range of 0.4% to 0.8%. The average first crack tensile strength was 1.75 MPa, and the final tensile strength was 1.9 MPa, about 9% higher. So, the short fibers reinforcement was able to successfully bridge the cracked matrix with new fine cracks formation.

Based on this context, this work investigated the mechanical behavior of cementitious materials reinforced with piassava and jute short fibers, focusing on the fiber-matrix interface. The interface was evaluated using the indirect method by plates' flexural tests. Furthermore, after the mechanical tests, fractographic analyzes were performed, aiming to understand the fracture surface of the tested samples. The present study proposed to comprehend the failure mechanisms of natural fibers by image analysis after the composite failure regarding the fiber-matrix interface.

MATERIALS AND METHODS

The piassava fibers were bought in the Ver-o-Peso fair (Belém city, Pará state, Brazil), in their natural form as bundles of 4 m length, approximately. The jute fibers were acquired as fabrics, made by Companhia Têxtil de Castanhal (Castanhal city, Pará, Brazil). The fibers were manually cut, and a fixed length of about 15 mm was adopted. Fig. 2 presents images of the already cut fibers and their respective surface/shape analyzed by a stereoscope microscope (SMZ800N, Nikon). The jute fibers presented a multi-filaments arrangement, as twisted yarn, while piassava fibers look like natural monofilaments with a stiff appearance. The mechanical and morphological characteristics of these fibers are summarized in Table I.

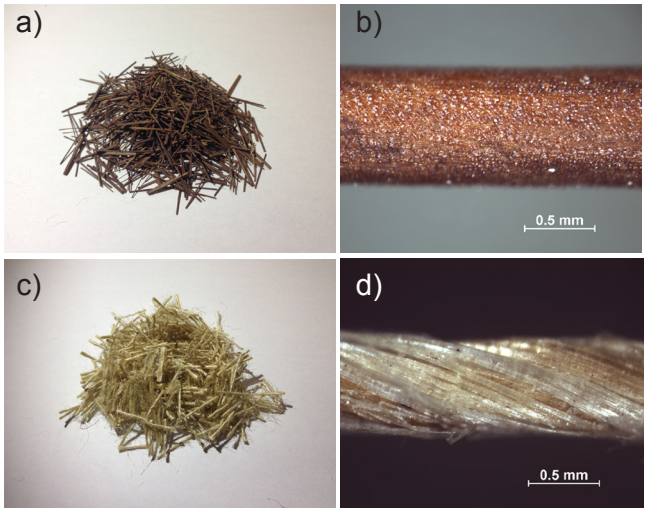

Figure 2: Images of the piassava (a,b) and jute (c,d) fibers cut with a length of 15 mm; details of a piassava single fiber surface (b) and the twisted yarn shape of a jute fiber (d) are shown.

Table I - Mechanical and morphological characteristics of piassava and jute fibers [24, 25, 36-38].

Characteristic	Piassava	Jute
Tensile strength (MPa)	134-143	320-800
Young's modulus (GPa)	1.07-4.59	26.5-37.5
Strain-to-failure (%)	5.0-21.9	1.5-2.5
Diameter (μm)	1100	18-200
Density (g/cm^3)	1.4	1.3-1.5
Moisture (%)	-	12.5-17.0

The mortar matrix was designed with the ratio of 1:2:0.5 (cement:sand:water); Portland cement CPII-F 32 (Lafarge Holcim) and commercial sand employed to supply the construction industry at the Belém city was used. The average compressive strength of the mortar matrix after 28 days was 29.5±2.6 MPa based on the axial compressive test. According to the Brazilian standard NBR 16697/2018 [39], this cement should have a minimum compressive strength of 32 MPa at 28 days (mixing cement, specific sand, and water in a proportion of 1:3:0.48), proven by laboratory tests for the batch used (Table II). In addition to the mechanical characteristics, chemical tests were carried out with this cement batch, and the results are shown in Table III. It is worth mentioning the characteristics of the quartz sand used for the experimental program. The sand had a maximum size of 1.2 mm with a fineness modulus of 1.55. The granulometric curve of the sand is shown in Fig. 3 and its fine granulometry can be graphically observed.

Table II - Compressive strength (MPa) for the cement batch used.

Curing time	Mean±standard deviation	Standard specification*
1 day	13.4±1.6	Not applicable
3 days	22.5±1.0	≥ 10
7 days	27.6±1.2	≥ 20
28 days	34.9±1.0	≥ 32

** NBR 16697/2018.*

Table III - Results of chemical tests for the cement batch used.

Test	Brazilian standard	Mean	Standard specification*
$PF_{950ºC}$ (%)	NM18/12	5.83	≤ 6.5
SO_3 (%)	NM16/12	2.40	≤ 4.0
RI (%)	NM22/04	1.38	< 2.5
CaO_{Free} (%)	NM13/13	1.67	Not applicable
MgO (%)	NM14/12	1.81	≤ 6.5

** NBR 16697/2018; $PF_{950ºC}$: test to characterize loss on ignition (between 900 and 1000 ºC); RI: insoluble residue content.*

The total amount of fibers per specimen corresponded to a volume fraction of 1%. The cement and sand were firstly dry mixed for 1 min, and then water was added (mixed 3 min more). After the homogenized mortar mixture, the fibers were added and mixed for 2 min. The composite specimens reinforced by piassava (named P15) and jute (J15) for flexural tests were vibrated for 10 s on a vibratory table for better densification. All the specimens were cured in the molds for 24 h and then underwater for 28 days. Reference specimens without fibers (MTRX) were made for comparison. It is worth mentioning that the 1% of volume fraction had the main purpose of understanding the failure mechanisms at the fiber-matrix interaction during loading, which was analyzed by scanning electron microscopy (SEM). The specimens

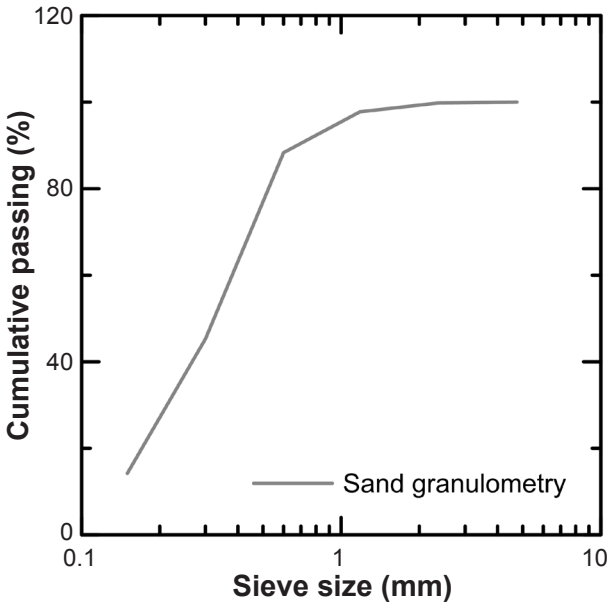

Figure 3: Granulometric curve of the sand.

were formed as plates, measuring 300 mm in length, 100 mm in width, and 25 mm in thickness [40]. Flexural tests were performed in a mechanical testing machine (WDW-100E, Arotec) controlled by a displacement rate of 0.5 mm/min with a 250 mm span between end supports. Five specimens per group (P15, J15, and MTRX) were tested in flexure. The materials' flexural strength (σ) and strain (ε) were determined according to the ASTM C1341 standard [41], following the Eqs. A and B, respectively:

$$\rho = \frac{3P.L}{2b.d^2} \quad (A)$$

$$\varepsilon = \frac{6D.d}{L^2} \quad (B)$$

where P is the force at a given point in the test (N), L is the outer support span (mm), D is the deflection at beam center at a given point in the test (mm), b is the test specimen width (mm), and d is the test specimen thickness (mm). After cracking and reaching the load peak, the samples remained under constant loading in order to acquire the residual strength of the cementitious composite. In the next step, their fracture surfaces were examined using a tabletop electron microscope (TM 3000, Hitachi). For the surface analysis, the fractured specimens were cut into pieces measuring about 25 mm in length by 25 mm in width, limited by the equipment sample holder.

RESULTS AND DISCUSSION

Mechanical properties: both the P15 and J15 presented the flexural softening behavior, with a single crack opening bridged by their fibers. This behavior can be explained by the volume fraction used (1%), which was considered insufficient to provide the flexural hardening behavior [32].

Fig. 4 shows the materials' mechanical behavior under flexural tests, considering not only the flexural strength by strain but also the toughness by center deflection. Comparing the composites' performance, J15 presented strength 13% lower than P15, but strain 3% higher. Contrasting the composites to MTRX, P15 presented strength 4% higher

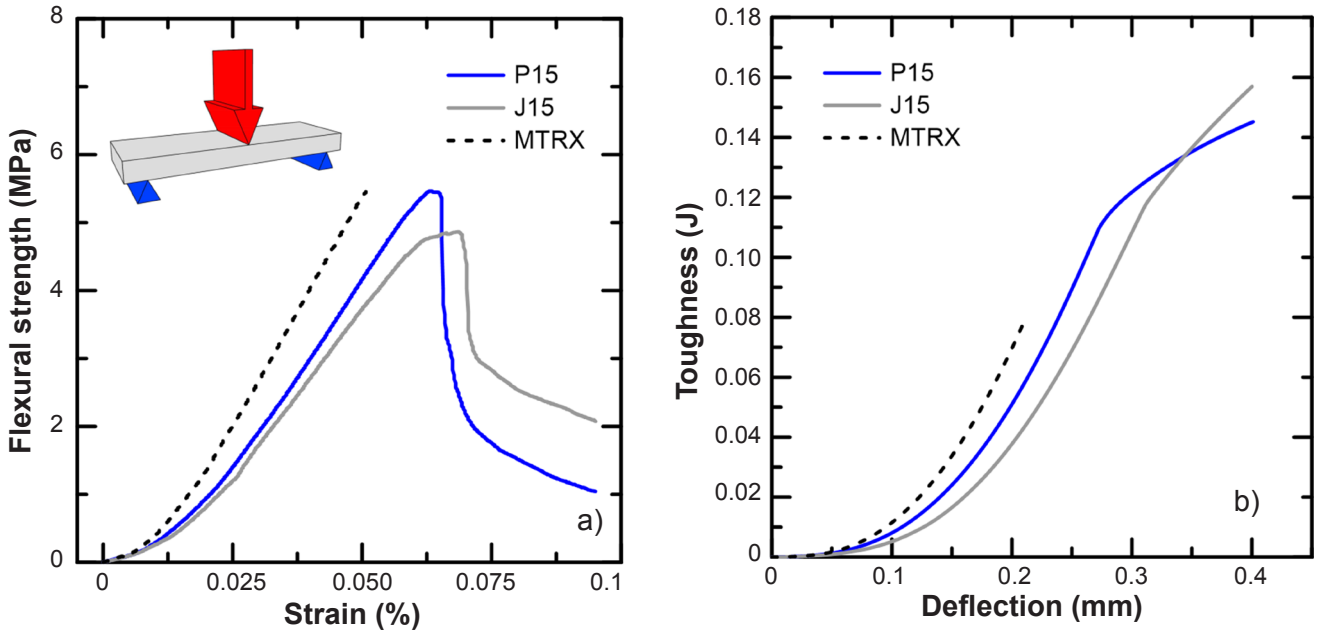

Figure 4: Mechanical behavior of the materials under flexural tests (a) and its toughness along with deflection (b).

Table IV - Mechanical properties of the materials under flexural tests.

Specimen	Strength (MPa)	Strain (%)	Modulus (GPa)	Toughness (J)
MTRX	5.43±0.24	0.051±0.001	0.140±0.003	0.079±0.008
P15	5.71±0.39	0.066±0.002	0.122±0.011	0.145±0.003
J15	5.07±0.09	0.068±0.005	0.107±0.004	0.157±0.012

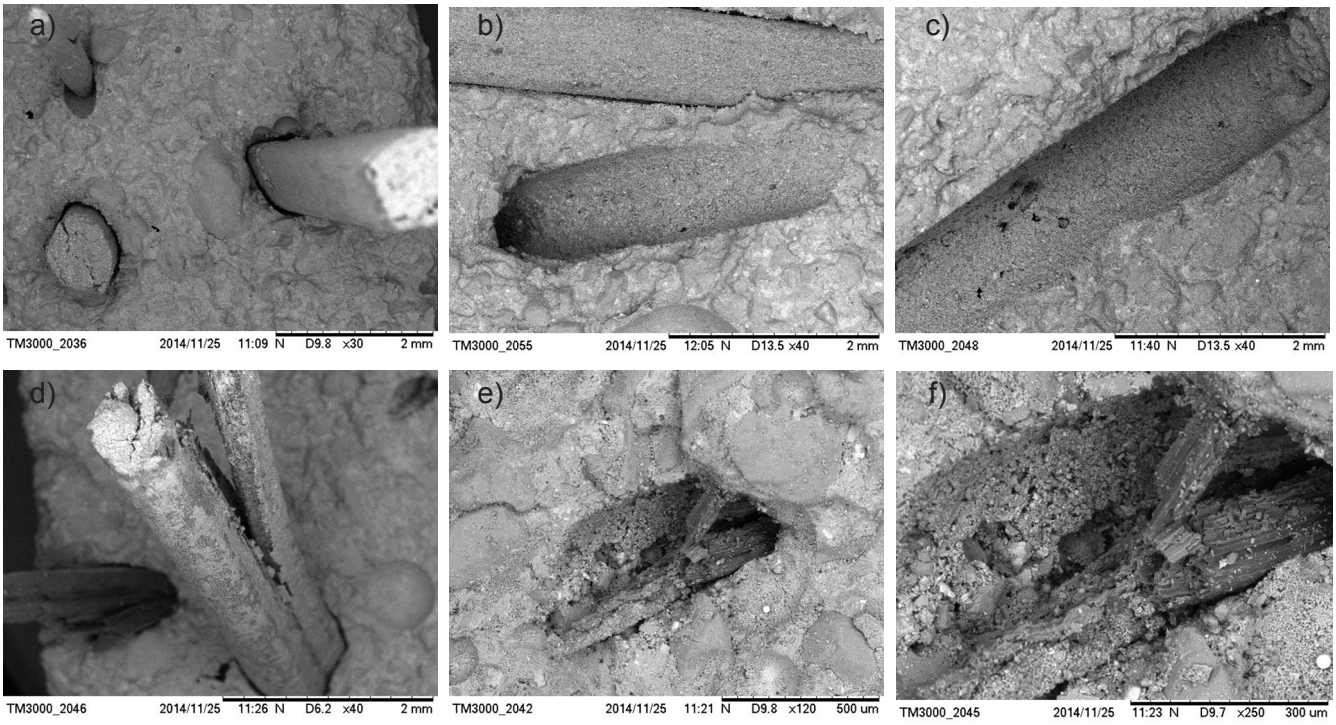

Figure 5: Fractographic images of composites reinforced by piassava fibers (P15).

while J15 was 7% lower, which in this case corroborated the fibers' wispy influence on their final resistance. Besides, it is possible to affirm that both P15 and J15 presented their maximum strength mostly ruled by the matrix mechanical properties once their strength peaks were restricted to the linear elastic zone. Their mechanical properties results are summarized in Table IV. About the strain, P15 and J15 presented enhancements around 29% and 33% over the MTRX, respectively. Even without a significant contribution to strength or a strain hardening behavior, the volume of fibers provided strain improvements before the first crack formation, and consequently, a higher capacity of energy absorption. This can be explained by the toughness graph that showed a higher gradient of toughness by deflection for both composites when compared to the matrix response, reaching almost twice the result found for the MTRX sample as is presented in Fig. 4b. Although the P15 presented higher flexural strength by the peak load, the J15 composite presented higher toughness at 0.4 mm deflection. The J15 residual strength ruled the toughness response, reaching 2 MPa at 0.1% strain while P15 reached 1 MPa.

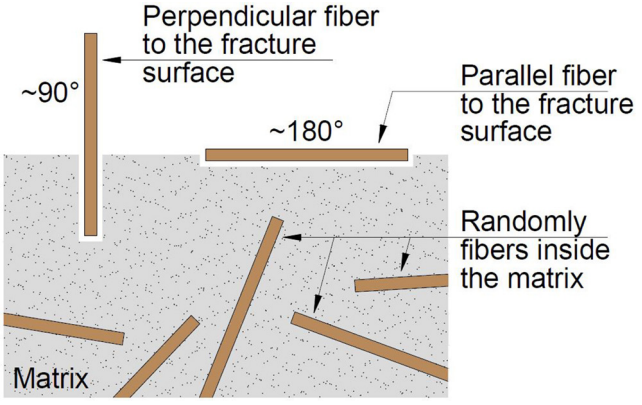

Figure 6: Schematic illustration of the fiber's orientation in the matrix.

Fractography: through SEM images, it was possible to analyze the consequences of fiber structure and its interface with the matrix during the cracking mechanisms. It is worth reiterating that the used discrete piassava and jute fibers were randomly arranged inside the composite, which provided different fiber angles on the fracture surface. Fig. 5a shows a piassava fiber perpendicularly oriented to the fractured surface, which probably represented the highest mechanical efficiency due to the alignment of the fiber with respect to the loading direction. According to Naaman [42], the alignment of the fiber with respect to the loading direction increases both the fiber pullout load and the response at the ultimate load. Fig. 5b presents a pulled-out fiber's cavity exhibiting an orientation angle between 45° and 90°. In both cases, it is possible to assume that the piassava fibers provided stress bridging during the cracking process, unless for cases where fibers are completely parallel to the fracture surface as it is shown in Fig. 5c. In this context, the fiber did not work as a stress-transfer bridge but perhaps represented a weak point during the crack formation, contributing to its propagation. Fig. 5d shows a failed piassava fiber, possibly by shear stress, which may indicate a reasonable fiber-matrix adhesion. The same adhesion can be noted in Figs. 5e and 5f, which present a broken fiber after the crack opening feasibly associated with good mechanical anchoring. This P15 behavior was associated with the mechanical and morphological characteristics of piassava fibers, which presented a low

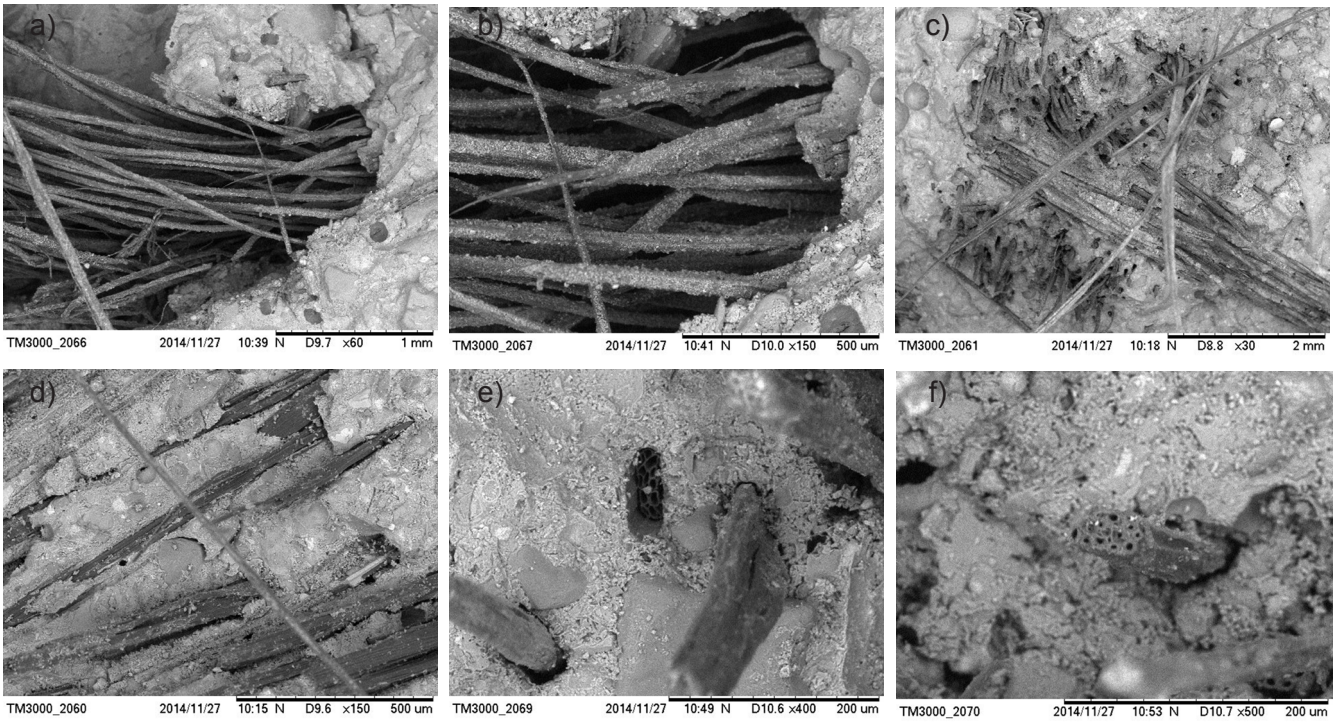

Figure 7: Fractographic images of composites reinforced by jute fibers (J15).

Young's modulus and a surface marked by a regular array of silicon-rich star-like protrusions, which could help their mechanical interlock [43]. It may justify the P15 higher stiffness over J15. For a better understanding of fibers orientation on cracking mechanics, Fig. 6 schematically illustrates the relationship between the fibers' angles and the fracture surface.

The jute fibers, used as twisted yarn, presented two different fiber-matrix interaction results. Figs. 7a and 7b show a collapse at the yarn arrangement by jute filaments segregation, which caused voids inside the matrix. This segregation may be explained by the fiber volume variation after water contact, increasing its volume due to the filling of its micro-cavities and subsequently decreasing by losing the water retained to the matrix during its curing. These kinds of voids can be considered material structure imperfections, acting as cracking propagators, which may be responsible for the J15 lower flexural strength. On the other hand, Figs. 7c and 7d present the same segregation of jute filaments, but in this case, there was a significant filling of the matrix between the voids. Figs. 7e and 7f show jute monofilaments dispersed in the matrix. This separation probably occurred mechanically, during the mixing of the materials. In these images, it is possible to identify the lumens (internal fiber cavities like tube shapes) that correspond to the microfibers [28, 44].

CONCLUSIONS

As expected, the composites presented flexural-softening behavior due to their low fibers' volume (1%), which not significantly influenced their flexural strength but reasonably enhanced their strain capacity. The image analysis showed the fibers' orientation influence at the cracking region, especially when fibers presented high stiffness, such as piassava. It was possible to notice that, when favorably oriented, the piassava fibers demonstrated significant adherence, failing due to shear or total rupture. This behavior may have contributed to the lower residual strength of the composite, when compared to the composite reinforced with jute fiber, even resulting in a lower toughness. The jute fiber, which was used as twisted yarn, provided voids to the composite, making it impossible to fully cover the fiber with the cementitious mortar. These kinds of voids can be considered material structure imperfections, acting as cracking propagators, which may be responsible for the J15 lower flexural strength. However, from the fractography, a considerable dispersion of monofilaments in the mixture was seen, which may have occurred mechanically during the mixing process. These monofilaments must have contributed to a residual stress response greater than the case of the piassava fiber since the dispersed monofilaments can control the propagation and opening of the cracks more effectively. Therefore, as much as the voids generated by the jute yarns reduced the maximum load, the dispersed monofilaments contributed to greater residual strength, and consequently to a greater toughness. The results showed that the morphology of natural fibers and their orientation in the matrix can be decisive for the mechanical behavior of the composite. In this study, fiber failure due to good adhesion, pullout, and the formation of voids harmful to the matrix (due to twisted shape in the case of jute) were noted. Through the type of failure of each fiber, it was possible to clarify the variation in the mechanical behavior of the composite plates. Finally, there is a need to investigate some factors that can significantly influence the properties of mortar plates reinforced with discrete fibers. The scaling effect is one of these, which can consider not only sample thickness but also its length, reaching larger spans in bending. Another point is the volume of discrete fibers used as reinforcement since better post-peak properties can be achieved with the volume increase of fibers. Furthermore, durability is also an important issue for cementitious composites reinforced with natural fibers since the fibers can be degraded even by cement hydration products. Therefore, more points should be addressed in further research.

ACKNOWLEDGMENT

This study was financed in part by the Coordenação de Aperfeiçoamento de Pessoal de Nível Superior - Brasil (CAPES) - Finance Code 001.

REFERENCES

[1] P.J.M. Mehta, P.K. Monteiro, *Concrete: microstructure, properties, and materials*, 3rd ed., McGraw-Hill, New York (2006).
[2] P. Bartos, Int. J. Cem. Compos. **3** (1981) 159.
[3] K. Georgiadi-Stefanidi, E. Mistakidis, D. Pantousa, M. Zygomalas, Constr. Build. Mater. **24** (2010) 2489.
[4] A.E. Naaman, J. Adv. Concr. Technol. **1** (2003) 241.
[5] Y.-C. Ou, M.-S. Tsai, K.-Y. Liu, K.-C. Chang, J. Mater. Civ. Eng. **24** (2012) 207.
[6] D.A. Fanella, A.E. Naaman, ACI J. Proc. **82** (1985) 475.
[7] R.J. Gray, C.D. Johnston, Int. J. Cem. Compos. Light. Concr. **9** (1987) 43.
[8] M. Maage, Mat. Constr. **10** (1977) 297.
[9] Y. Chan, Adv. Cem. Based Mater. **5** (1997) 8.
[10] M.J. Shannag, R. Brincker, W. Hansen, Cem. Concr. Res. **27** (1997) 925.
[11] V. Li, Adv. Cem. Based Mater. **6** (1997) 1.
[12] Y. Lee, S.T. Kang, J.K. Kim, Constr. Build. Mater. **24** (2010) 2030.
[13] R.J. Gray, Int. J. Adhes. Adhes. **3** (1983) 197.
[14] C. DiFrancia, T.C. Ward, R.O. Claus, Compos. Part A Appl. Sci. Manuf. **27** (1996) 597.
[15] V.A.M. Monteiro, L.R. Lima, F.S. Silva, Constr. Build. Mater. **188** (2018) 280.
[16] Y. Wang, V.C. Lf, S. Backer, Int. J. Cem. Compos. **10** (1988) 143.
[17] Z. Lin, T. Kanda, V.C. Li, J. Concr. Sci. **1** (1999) 173.
[18] V.N. Lima, D.C.T. Cardoso, F.A. Silva, J. Mater. Civ. Eng. **33**, 8 (2021) 1.

[19] P.W.R. Beaumont, J.C. Aleszka, J. Mater. Sci. **13** (1978) 1749.
[20] R.S. Castoldi, L.M.S. de Souza, F.A. Silva, Constr. Build. Mater. **211** (2019) 617.
[21] F.P. Teixeira, F.A. Silva, Cem. Concr. Compos. **114** (2020) 103775.
[22] A. Kicińska-Jakubowska, E. Bogacz, J. Małgorzata, J. Nat. Fibers **9** (2012) 150.
[23] M.E.A. Fidelis, T.V.C. Pereira, O.D.F.M. Gomes, F.A. Silva, R.D. Toledo Filho, J. Mater. Res. Technol. **2** (2013) 149.
[24] A. Komuraiah, N.S. Kumar, B.D. Prasad, Mech. Compos. Mater. **50** (2014) 359.
[25] L. Yan, B. Kasal, L. Huang, Compos. B Eng. **92** (2016) 94.
[26] J. Yu, N. Paterson, J. Blamey, M. Millan, Fuel **191** (2017) 140.
[27] S.A. Ovalle-Serrano, F.N. Gómez, C. Blanco-Tirado, M.Y. Combariza, Carbohydr. Polym. **189** (2018) 169.
[28] F.P. Teixeira, O.F.M. Gomes, F.A. Silva, BioResources **14** (2019) 1494.
[29] L.O. de Souza, L.M.S. Souza, F.A. Silva, Mag. Concr. Res. **73** (2019) 135.
[30] J.D.A.M. Filho, F.D.A. Silva, R.D. Toledo Filho, Cem. Concr. Compos. **40** (2013) 30.
[31] A.L.S. d'Almeida, J.A. Melo Filho, R.D. Toledo Filho, Chem. Eng. Trans. **17** (2009) 1717.
[32] D.G. Soltan, P. das Neves, A. Olvera, H. Savastano Junior, V.C. Li, Ind. Crops Prod. **103** (2017) 1.
[33] A.P. Fantilli, H. Mihashi, P. Vallini, Cem. Concr. Res. **39** (2009) 1217.
[34] C.L. Hwang, V.A. Tran, J.W. Hong, Y.C. Hsieh, Constr. Build. Mater. **127** (2016) 984.
[35] B. Zukowski, F.A. Silva, R.D. Toledo Filho, Cem. Concr. Compos. **89** (2018) 150.
[36] D.B. Dittenber, H.V.S. Gangarao, Compos. Part A Appl. Sci. Manuf. **43** (2012) 1419.
[37] O. Onuaguluchi, N. Banthia, Cem. Concr. Compos. **68** (2016) 96.
[38] A. Elzubair, C.M. Chagas Bonelli, J.C. Miguez Suarez, E.B. Mano, J. Nat. Fibers **4** (2007) 13.
[39] NBR 16697, "Cimento Portland: requisitos", ABNT (2018).
[40] M.N.P.B. Peres, S.F. Martins Neto, R.T. Fujiyama, Rev. Engren. **2** (2012) 99.
[41] C1341-13, "Standard test method for flexural properties of continuous fiber-reinforced", ASTM Int. (2013).
[42] A.E. Naaman, "A statistical theory of strength for fiber reinforced concrete", Ph.D. Thesis, Massachusetts Inst. Technol. (1972).
[43] J.R.M. d'Almeida, R.C.M.P. Aquino, S.N. Monteiro, Compos. Part A Appl. Sci. Manuf. **37** (2006) 1473.
[44] F. Martins, F.P. Teixeira, J.F. Lima, F.A. Silva, in Proc. 4th Braz. Conf. Compos. Mater., PUC, Rio Janeiro (2018).
(Rec. 07/05/2021, Rev. 03/08/2021, Ac. 12/09/2021)